Scientific Research

Research on Key Technologies of Prefabricated Assembled Construction Nodes for Shanghai Riverside Channel

Fuqiu Yin [1,*], Xiangke Chen [1], Yi Zhou [2] , Xiaofeng Wang [3] and Xiabin Yuan [4]

1 Shanghai Chengtou Highway Investment (Group) Co., Ltd., Shanghai 200335, China;
2 Shanghai Tunnel Engineering Co., Ltd., Shanghai 200032, China;
3 Shanghai Urban Construction Municipal Engineering (Group) Co., Ltd., Shanghai 200032, China;
4 Shanghai Swissdam Environmental Protection Technology Co., Ltd., Shanghai 200080, China;
* Correspondence: 85052717@qq.com

Abstract: In recent years, the use and promotion of prefabricated assembly construction in China have been rapidly advancing, especially when combined with prestressing technology and Ultra High Performance Concrete (UHPC) as a new material to solve the connection and node construction between assembly components. It has started to be widely applied in developed coastal areas of China. This paper focuses on the node connection part of the prefabricated assembly construction used in the Shanghai Riverside Channel project. It explores the application of UHPC material in the assembly process and verifies the reliability of the relevant connection nodes through various experiments. The successful application of this research has been implemented in the Shanghai Riverside Tunnel project.

Keywords: Prefabricated assembly; UHPC; connection node; pull-out test; wet joint

Citation: Yin, F.; Chen, X.; Zhou, Y.; Wang, X.; Yuan, X. Research on Key Technologies of Prefabricated Assembled Construction Nodes for Shanghai Riverside Channel. *Prestress Technology* **2023**, *3*, 30-43. https://doi.org/10.59238/j.pt.2023.03.003

Received: 6/12/2023
Accepted: 15/12/2023
Published: 25/12/2023

1 Introduction

Due to its characteristics of fast speed, high efficiency, and good stability in quality, prefabricated assembly has become increasingly applied in various construction projects. Its convenience in coordinating construction organization and scheduling allows for the optimization of the process flow within the shortest possible time. Simultaneously, it enables a comprehensive consideration in tandem with the design [1-3].

Figure 1 Precast assembly bridge

The projects are divided based on their construction advantages and have the following salient characteristics:

(1) Open traffic express: With the increasing pressure on urban traffic in China in recent years, this pressure not only seriously affects the quality of road traffic

but also has a greater impact on the normal service life of roads. To improve road quality and traffic safety, maintenance must be carried out. However, traditional maintenance methods affect roads for a long time and slow traffic. The main reason is that the repair process is complicated, and post-maintenance is troublesome. In contrast, a precast assembly has assembly panels prepared in advance, and the grid can be opened to traffic after simple assembly during the construction process without delaying the normal use of the road or causing traffic jams.

(2) Savings in maintenance costs: Compared with traditional construction techniques, precast materials are less expensive and have a wider range of sources. The main materials used are ordinary Portland cement and steel bars, which can greatly reduce construction costs. Moreover, precast and decentralized installation can be used to reduce various additional costs for site construction, improve road traffic efficiency, and achieve greater economic and social benefits.

(3) Good durability: Traditional construction technologies mainly use concrete, but concrete itself has variable characteristics and is more difficult to conserve in later stages of useful service life. Once the maintenance cannot keep up, the material is prone to a decrease in quality, which affects its service life. Depot concrete is mainly used for precast slabs and has the advantages of multiple maintenance methods and low maintenance costs. In addition, the overall durability of a road can be improved by adding corrosion-resistant or acid and alkali-resistant components, thereby extending the service life.

In a fully precast bridge, the superstructure and substructure are precasted in a factory and assembled on site. The structural components of all-precast bridges, which have long maintenance times, strong corrosion resistance, and high structural quality, are produced in factories. The bent caps, pier columns, bridge decks and anti-collision walls can all be precasted in the factory and then assembled on site [4,5].

Ultrahigh-performance concrete (UHPC) was first developed in the early 1980s and has since been used where special strength and durability are needed. UHPC has become the most innovative cement-based engineering material in recent years. It has excellent material properties compared to ordinary concrete. Therefore, UHPC will be a trending topic of research and application in the building materials industry for a long time [3,6].

Compared with traditional concrete, UHPC is structurally closer to steel. Therefore, the material needed for the structure to meet the same requirements is reduced by 70%. When used in bridge decks, UHPC can reduce the overall structure weight, reduce substructures, and reduce transportation and installation costs.

Figure 2 UHPC structural failure surface

UHPC is a high-strength, high-toughness, work-oriented concrete developed by the comprehensive use of cement-based composite technology, fluid concrete technology, micro-expansion concrete technology, interface modification technology, hybrid fiber technology, and anti-settlement and anti-bleeding technologies. Cement-based composite materials offer excellent performance and durability. Its high performance is derived from the carefully calibrated material-to-component ratio and mixing sequence, which tightly aggregate the molecules together to form a very tight bond. This high packing density results in excellent flexural, compressive and impact strength. Because the molecules are tightly packed, the capillary pores that exist in conventional concrete are eliminated. UHPC is self-flowing and dense forming, offering good interface bond strength with old concrete and steel rebar and strong corrosion resistance. Currently, UHPC120~UHPC180 series products are in use.

Moreover, UHPC is suitable for engineering applications such as precast component fabrication, bridge wet joint connections, bridge pier-column connections, steel bridge deck pavement, maintenance and reinforcement, building curtain walls, and siding.

2 Application Study of UHPC at the Precast Node

2.1 Material Performance Verification

2.1.1 Construction Performance

UHPC has excellent construction performance, with a flow dilation of 800 mm, indicating excellent fluidity and workability during construction. As shown in Figure 3, UHPC fully meets the construction process requirements.

Figure 3 UHPC excellent fluidity and workability performance

2.1.2 Mechanical Properties

UHPC mechanical properties include cubic compressive strength, elastic modulus and tensile strength. After standard maintenance for 28 d, the compressive strength and tensile strength reach 158.59 MPa and 13.63 MPa, respectively, which are comparable to the values obtained for steam-cured concrete. The elastic modulus of UHPC can reach 48.5 GPa, which indicates good rigidity and improved deformation synergy.

Table 1 UHPC mechanical properties (Unit: MPa)

Maintenance method	Compressive strength	Elastic modulus	Tensile strength
Steam maintenance	160.7±5.3	48.6±0.8	13.86±0.51
28 d standard maintenance	158.5±12.62	48.5±0.5	13.63±0.76

https://doi.org/10.59238/j.pt.2023.03.003

2.1.3 Long Term Deformation

A study on the long-term deformation performance of UHPC along a river was carried out [7]. Considering that the shrinkage of the UHPC system is mainly autogenous shrinkage, an autogenous shrinkage performance test was carried out, and the results were obtained from the setting of the concrete. Figure 4 shows that the contraction of UHPC developed rapidly in the early stage and stabilized in the later stage, and the UHPC 70 d autogenous shrinkage value was 192 E-6. The hyperbolic function was used to fit the autogenous shrinkage data from the mathematical expression of concrete shrinkage in the ACI, and the function was:

$$\varepsilon_{sh}(t) = \varepsilon_{shu}\frac{t}{A+t} \tag{1}$$

where ε_{shu} is the final shrinkage value and A is a constant related to the development trend of shrinkage.

The final fitting value of UHPC, ε_{shu}, was 215 E-6, which met the design indicators, exhibited good volume stability, and significantly reduced the risk of cracking during the construction process. The craft provides a feasible route.

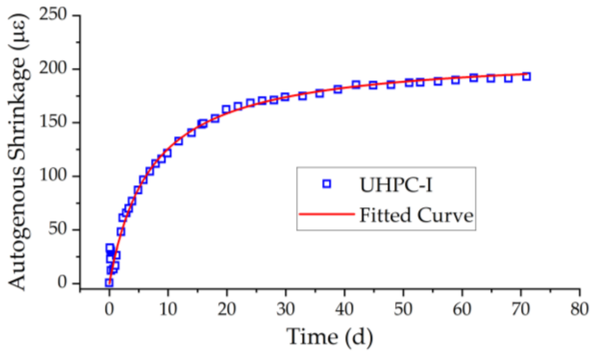

Figure 4 UHPC shrinkage performance

The results of the UHPC compression creep test are shown in Figure 5. The compression creep coefficient of UHPC is closely related to the loading age; the later the loading age is, the smaller the compression creep coefficient is. This is due to the relatively small degree of early hydration of the concrete.

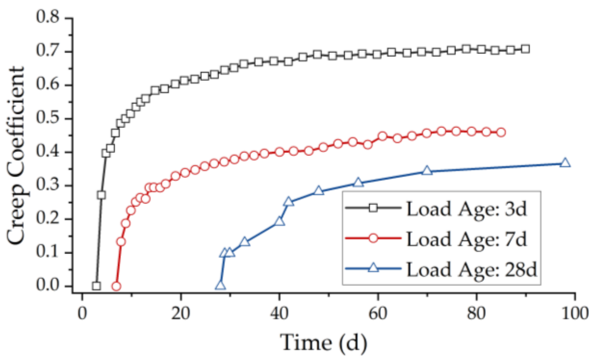

Figure 5 UHPC creep performance

2.1.4 Durability Performance

(1) Water infiltration resistance

The tests were conducted with reference to the water seepage height method specified in the "Standard for Test Methods for Long-term Performance and Durability of Ordinary Concrete" (GB/T 50082-2009). The water seepage heights of the

UHPC specimens are shown in Table 2. The table shows that the water seepage height of the UHPC was 0 mm.

Table 2 UHPC water seepage height (Unit: mm)

Maintenance method	Water seepage height
Steam maintenance	0.00
28 d standard maintenance	0.00

(2) Resistance to chloride ion infiltration

The tests were performed with reference to the rapid chloride ion transfer coefficient method (or RCM method) specified in the "Standard for Test Methods for Long-term Performance and Durability of Ordinary Concrete" (GB/T 50082-2009), and the chloride ion diffusion coefficient of the UHPC (steel fiber removal) matrix is shown in the Table 3. It can be seen in the table that the chloride ion diffusion coefficient of UHPC was less than $0.01 \times 10^{-12}\ m^2/s$, indicating excellent compactness.

Table 3 Chloride ion diffusion coefficients of UHPC (Unit: $10^{-12}\ m^2/s$)

Maintenance method	Chloride ion diffusion coefficient
Steam maintenance	< 0.01
28 d standard maintenance	< 0.01

(3) Carbonization performance

The carbonation performance test was performed with reference to the carbonation test specified in the "Standard for Test Methods for Long-term Performance and Durability of Ordinary Concrete" (GB/T 50082-2009). The carbonation depths of UHPC under standard maintenance conditions after 3 d, 7 d, 14 d and 28 d are shown in Table 4. The table shows that the carbonization depth of UHPC after carbonization for 28 days is still < 0.1 mm.

Table 4 Carbonization performance of UHPC (Unit: mm)

Time	Carbonization depth	Time	Carbonization depth
3d	0.0	14d	0.0
7d	0.0	28d	< 0.1

(4) Freeze–thaw resistance

The freeze–thaw resistance of UHPC was tested according to the quick-freezing method specified in the "Standard for Test Methods for Long-term Performance and Durability of Ordinary Concrete" (GB/T 50082-2009), and the freeze–thaw resistance of UHPC is shown in Table 5. The table shows that UHPC underwent 20 freeze–thaw cycles with basically no mass loss.

Table 5 Freeze–thaw resistance performance of UHPC

Maintenance method	Result
Standard maintenance	Almost no mass loss after 20 freeze–thaw cycles
Heat maintenance	Almost no mass loss after 20 freeze–thaw cycles

(5) Self-compacting property

UHPC has good self-compacting performance and can self-level and compact under the action of its own gravity. Even if there are dense steel bars inside the perfusion cavity, the cavity can be completely filled without vibration.

Figure 6 The compactness of the formed specimen is good after cutting

2.2 *Structural Performance Verification*

2.2.1 Rebar Pullout Test

The results of the rebar pullout test are shown in Table 6, and the typical failure modes are shown in Figure 7. The test results show that UHPC has excellent grip strength and wrapping ability and can ensure tensile failure of the rebar when the burial depth of the 12~20 mm rebar is 3×d. d is the diameter of the rebar.

Table 6 Results of the rebar pullout test

Plane size of specimen (mm×mm)	Rebar diameter (mm)	Anchorage length L=n×d	Damage mode (Unit)
150×150	12	3d,4d	Rebar fracture
150×150	16	3d,4d	Rebar fracture
150×150	20	3d,4d	Rebar fracture
150×150	25	4d	Rebar fracture
150×150	28	4d	Rebar fracture
150×150	32	5d	Rebar fracture

Figure 7 Typical forms of rebar pullout failure

2.2.2 Static Test of the Joint Plates

Figure 8 shows the load–deflection curve of specimens. The responses of two identical plates are close to each other before cracking but are slightly different after cracking. Before cracking, the component response was linear; after cracking, the component stiffness decreased, and the deflection increased faster; after shear cracking, the component deflection increased more when the load increase was not large; and eventually, due to the small setting of the shear-span ratio of the component, the brittle shear failure mode increased. The main test results are summarized in Table 7. Due to the small setting of the shear-span ratio, all the specimens experienced shear failure. The cracking load and the nominal cracking stress of the cross-section of the two test plates with different joint forms were similar; the cracking load was approximately 200 kN, and the nominal cracking stress of the cross-section was approximately 12 MPa. However, the ultimate bearing capacity of the tongue and groove joint slab was 5.5% greater than the ultimate bearing capacity of the plain joint.

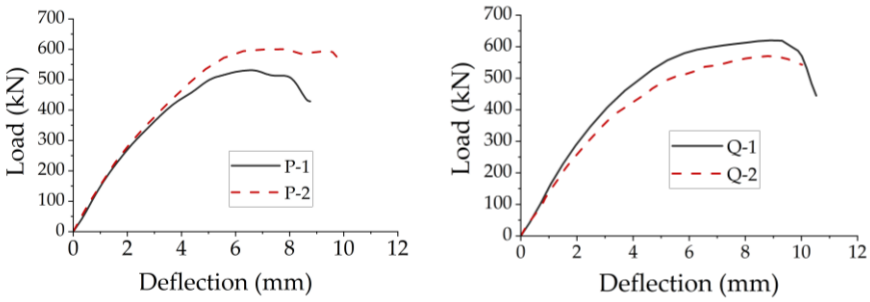

(a) flat plain joint (b) groove joint

Figure 8 Load–deflection curve of the test plate

Table 7 Summary of the main test results

Test No.	a/d	σ_u (MPa)	σ_{cr} (MPa)	V_u (kN)	V_m (kN)	V_{cr} (kN)	f_{max} (mm)	Damage mode
P-1	1.76	30.8	14.5	531.0	230	470	8.75	Shear failure
P-2	1.76	34.8	11.6	599.6	190	485	9.73	Shear failure
Q-1	1.76	36.1	13.9	621.3	240	494	10.52	Shear failure
Q-2	1.76	33.2	11.0	571.2	190	481	9.98	Shear failure

Note: a/d: shear-span ratio; σ_u: nominal ultimate stress on component tension side; σ_{cr}: nominal cracking stress on component; V_u: ultimate bearing capacity; V_m: flexural crack load; V_{cr}: shear cracking load; f_{max}: ultimate deflection of component.

Figure 9 shows the failure diagrams of all the specimens. All the components suffered diagonal-tension shear failure. Figure 10 shows the distribution of cracks in the test plates. Fewer UPCs and cracks develop near joints, and cracks mostly appear in ordinary concrete and develop completely, indicating that the joints have good load-bearing performance.

At the beginning of loading, the test panel was in the elastic stage, and the response was linear. When the load increased to approximately 40% of the ultimate load, the first flexural crack appeared near the bottom of the loading point at a height of approximately 1/4 to 1/3 of the cross-sectional height. As the load increases, a small number of new flexural cracks appear in the purely curved section of the midspan, but the development heights are not high. Cracks at the joints generally occur after the initial cracks in the components, indicating that the interfacial bonding performance at the joints is better. As the load increased to approximately 80% of the ultimate load, the first shear cracks, most of which were web shear cracks, appeared in the shear span and developed rapidly toward the support and loading points. Subsequently, the shear cracks developed rapidly, a number of microscale shear oblique cracks appeared nearby, and the component deflection increased. Eventually, the component undergoes shear failure.

https://doi.org/10.59238/j.pt.2023.03.003

 

(a) P-1 (b) P-2

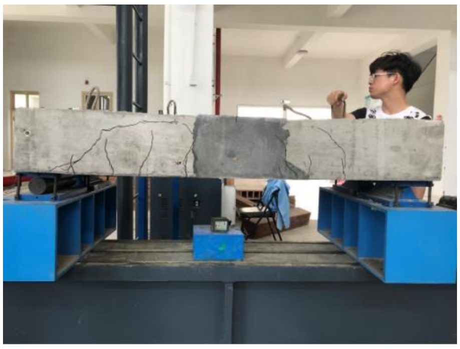 

(c) Q-1 (d) Q-2

Figure 9 Destruction diagram of test plates

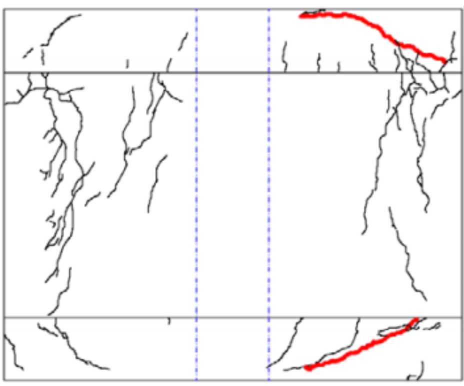 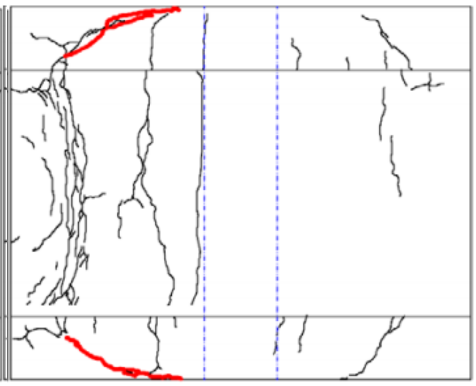

(a) P-1 (b) P-2

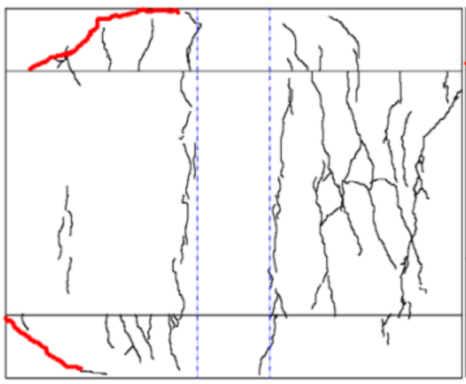 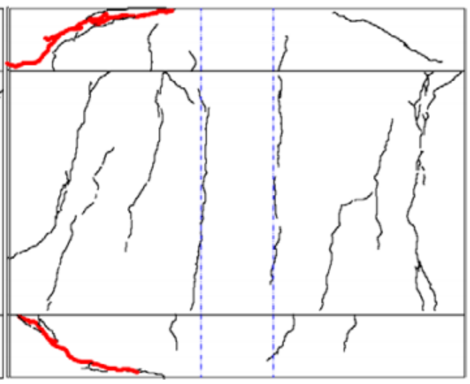

(c) Q-1 (d) Q-2

Figure 10 Distribution of cracks in test plates

2.2.3 Static Test of Pier–Column Joints

Figure 11 shows the load–deflection curve of specimens. The responses of the two components are similar. Before cracking, the component response was linear; after cracking, the component stiffness decreased, and the deflection increased faster; after shear cracking, the component deflection increased more when the load increase was not large; and eventually, due to the small setting of the shear-span ratio of the component, the brittle shear baroclinic failure mode was established. The main test results are summarized in Table 8. Due to the small shear-span ratio, all the specimens exhibited the shear baroclinic failure mode. The nominal cracking stress at the tension edge of specimens is approximately 16 MPa.

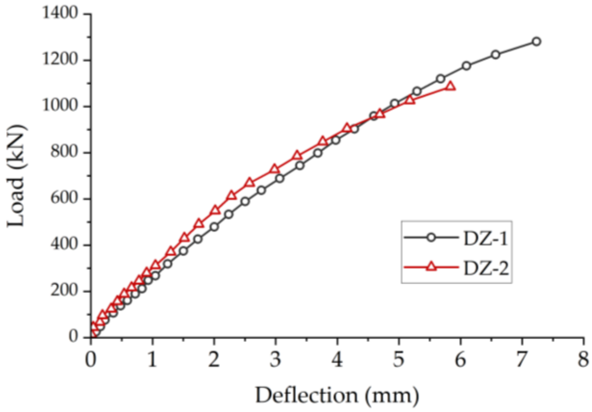

Figure 11 Load–deflection curves

Table 8 Summary of the main test results

Test No.	a/d	σ_u (MPa)	σ_{cr} (MPa)	V_u (kN)	V_m (kN)	V_{cr} (kN)	f_{max} (mm)	Damage mode
DZ-1	1.12	37.8	16.4	1275.2	552	700	7.24	Baroclinic failure
DZ-2	1.12	32.1	15.6	1084.9	528	-	5.85	Baroclinic failure

Note: a/d: shear-span ratio; σ_u: nominal ultimate stress on component tension side; σ_{cr}: nominal cracking stress on component; V_u: ultimate bearing capacity; V_m: flexural crack load; V_{cr}: shear cracking load; f_{max}: ultimate deflection of component.

Figure 12 shows the failure diagrams of all the specimens. All the components experienced shear baroclinic failure. Figure 13 shows the distribution of cracks in the test plates. UHPC joints exhibit fewer cracks, and cracks near the joints are less extensive. The majority of cracks tend to occur in regular concrete sections and are more pronounced, indicating favorable load-bearing performance of the joints.

At the beginning of loading, the specimen was in the elastic stage, and the response was linear. When the load reached approximately 45% of the ultimate load, the first flexural crack appeared approximately 30 cm outside the joint and was distributed symmetrically on both sides of the joint. As the load increases, a small number of new flexural cracks appear in the purely curved section of the midspan, but the development heights are not high. As the load increased to approximately 55% of the ultimate load, the first diagonal shear crack appeared in the shear span; this was a flexural-shear crack that developed to a very high height as soon as it appeared and developed rapidly toward the loading point. When the load increased to approximately 80% of the ultimate load, the joints were cracked, but the development was not high. Subsequently, the shear cracks developed rapidly, a number of microscale shear oblique cracks appeared nearby, a large area of concrete was crushed and spalled, and the component deflection increased. Eventually, the component underwent shear baroclinic failure.

 https://doi.org/10.59238/j.pt.2023.03.003

(a) DZ-1 (b) DZ-2

Figure 12 Fracture diagram of specimens

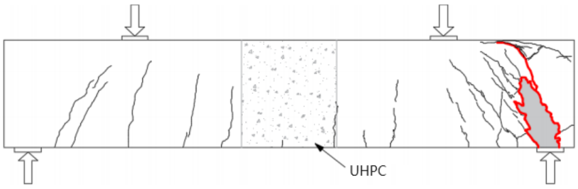

(a) DZ-1

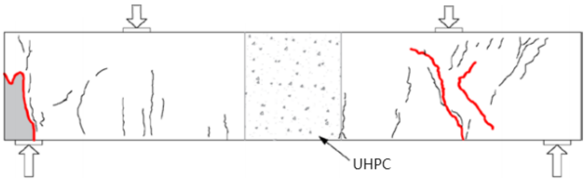

(b) DZ-2

Figure 13 Distribution of cracks in specimens

The test results verify that UHPC joints meet the needs of river channel projects, and all the indicators meet the design requirements.

3 Application of UHPC Joints for River Channels

The application of UHPC joints is primarily concentrated in critical junctures such as the connection between piers and abutments, the connection between piers and bent caps, wet joints in bridge deck plates, and wet joints in crash barriers. These key nodal points essentially encompass the current methods of UHPC application in prefabricated assembly bridge engineering. This plays a guiding and exemplary role in promoting the development of the UHPC industry.

3.1 UHPC Precast Case Study

(1) Connection between the pier column and pile cap

(a) Formwork installation (b) Formwork dismantling and concrete maintenance

Figure 14 Pier column and pile cap connection

(2) Connection between the pier column and bent cap

(a) Formwork and guardrail installation (b) Formwork dismantling and maintenance

Figure 15 Pier column and bent cap connection

(3) Wet joint connection of the bridge deck

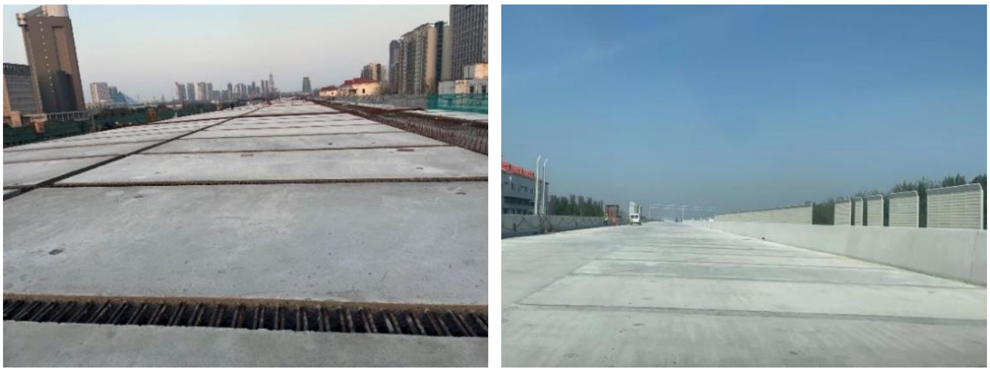

(a) Before forming wet joint (b) After forming wet joint

Figure 16 Wet joint connection of the bridge deck

(4) Wet joint connection of an anti-collision wall

(a) Before forming the wet joint (b) After forming the wet joint

Figure 17 Wet joint connection of an anti-collision wall

3.2 The Workflows of UHPC Precast Assembly Node Connections

The construction process of bridge UHPC precast assembly node connections can be divided into the following steps: foundation surface treatment → precast component hoisting → formwork design and installation → UHPC mixing, transportation and pouring → formwork removal and concrete maintenance.

 https://doi.org/10.59238/j.pt.2023.03.003

3.2.1 Foundation Surface Treatment

Before construction, the concrete surface was rinsed with a water gun to remove the floating ash and wet the concrete surface. Moreover, an angle grinder was used to descale and polish the steel bars.

3.2.2 Precast Component Lifting

Before the hoisting of precast components, the size and spacing of the reserved steel bars at the pile cap or foundation should be checked. Before the formal hoisting of columns, a trial lifting of the columns should be completed. The thickness of the steel spacers between the columns and the pile caps should be determined through trial lifting to reduce the adjustment time for formal hoisting. During the hoisting of the precast anti-collision wall and bridge deck, attention should be given to sealing the bottom gaps to prevent grout leakage from the UHPC during pouring.

3.2.3 Formwork Design and Installation

The formwork should be designed based on the actual size requirements at the site, have sufficient strength and stiffness, and be convenient for on-site installation. During installation, the stability and sealing performance of the formwork should be ensured to avoid mold running and grout leakage during the pouring process. Moreover, venting gaps were left in key parts to prevent cavities caused by the failure of internal air to be removed in time during the perfusion process and affecting project quality.

3.2.4 UHPC Mixing, Transportation and Pouring

Before mixing, we check whether the mixing equipment is in normal operation, the inner wall of the mixer remains wet, and no open water is allowed to remain; mixing is performed according to the construction mix ratio determined in the test. The concrete can only be discharged after the overall mixing is uniform, and powder and fiber agglomeration will not occur in the mixture. After stirring was complete, water or admixture was not added to the mixture. After the mixing is completed, the operator operates the equipment to transport the concrete to the construction area and opens the bin gate for pouring. The dual control standards of the design dimension and the slurry output from the grout hole were used for the grouting fullness. When the grout volume reaches the needed level and the grout hole overflows, pouring can be stopped, and the grouting area can be replenished 5 to 10 min after the completion of pouring to ensure that the grouting is full and dense.

3.2.5 Formwork Dismantling and Concrete Maintenance

When the 1 d strength of the maintenance test block under the same conditions in the field is greater than 35 MPa, the grout-retaining formwork and other temporary facilities can be removed.

After the UHPC is poured, the parts exposed to the air (inspection holes and perfusion holes) should be covered with health-preserving film for moistening and maintenance; when the health-preserving film is covered, the UHPC should not be damaged; during the moisturizing and maintenance process, inspection should be strengthened to check for water shortage. When there is a lack of water parts, should be timely replenishment of water conservation, and moisturizing maintenance should be continued for more than 3 days.

4 Conclusions

The Puxi junction section of the Shanghai River Channel was opened to traffic on November 25, 2022, which will greatly improve the road traffic efficiency of this route.

With improvements to domestic socioeconomic levels, the construction of engineering projects has developed toward higher, longer, and deeper angles and depths, which has placed greater requirements on the strength of concrete. At present, the production and construction methods of the construction industry are in the stage of restructuring and upgrading, and the Ministry of Construction is promoting the development of shop precast, new precasted integrated parts and assembly technology systems. Therefore, the demand for general concrete, high-performance concrete, and ultrahigh-performance concrete (UHPC) is increasing. UHPC helps to achieve light weight, high quality, high efficiency, and low resource consumption in building parts and components and can also be used for node connections of components to improve structural reliability and seismic resistance. Therefore, in the construction field, UHPC has good technological development potential and market development space [2].

Conflict of Interest: All authors disclosed no relevant relationships.

Data Availability Statement: The data that support the findings of this study are available from the corresponding author, Yin, upon reasonable request.

References

1. In Proceedings of the 26th East China Six Provinces and One City Civil Engineering Construction Technology Exchange Meeting, Hangzhou, 2020; pp. 709-713, doi:10.26914/c.cnkihy.2020.021305.
2. Zhang, H. On-site Installation and Positioning Technology of Prefabricated Columns for Shanghai Jiamein Elevated Project. *China Municipal Engineering* **2016**, 59-61+104, doi:10.3969/j.issn.1004-4655.2016.04.018.
3. Editorial Department of China Journal of Highway Transport. Review on China's Bridge Engineering Research:2021. *China Journal of Highway and Transport* **2021**, *34*, 1-97, doi:10.19721/j.cnki.1001-7372.2021.02.001.
4. Jia, J.; Guo, Y.; Song, N.; Zhu, Y.; Du, X.; Geng, L. Seismic Testing of Precast RC Bridge Pier Columns Anchored by Grouted Corrugated Ducts. *China Journal of Highway and Transport* **2018**, *31*, 211-220, doi:10.19721/j.cnki.1001-7372.2018.12.021.
5. Khaleghi, B.; Schultz, E.; Seguirant, S.; Marsh, L.; Haraldsson, O.; Eberhard, M.; Stanton, J. Accelerated bridge construction in Washington State: From research to practice. *PCI Journal* **2012**, 34-49.
6. Shao, X.; Fan, W.; Huang, Z. Application of Ultra-High-Performance Concrete in engineering structures. *China Civil Engineering Journal* **2021**, *54*, 1-13, doi:10.15951/j.tmgcxb.2021.01.001.
7. Xu, Y.; Liu, J.P.; Liu, J.Z.; Zhang, Q.Q.; Zhao, H.L. Creep at early ages of ultrahigh-strength concrete: experiment and modelling. *Mag Concrete Res* **2019**, *71*, 847-859, doi:10.1680/jmacr.17.00551.

AUTHOR BIOGRAPHIES

	**Fuqiu Yin** Prof. Engineer. Shanghai Chengtou Highway Investment (Group) Co., Ltd. Research Direction: Construction Management of Major Projects such as Bridges and Tunnels. Email: 85052717@qq.com		**Xiangke Chen** Prof. Engineer. Shanghai Chengtou Highway Investment (Group) Co., Ltd. Research Direction: Construction Management of Major Projects such as Bridges and Tunnels. Email: 150095957@qq.com
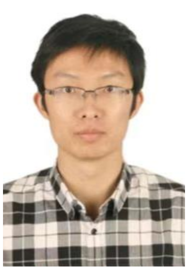	**Yi Zhou** Prof. Engineer. Shanghai Tunnel Engineering Co., Ltd. Research Direction: Highway or Municipal Engineering Project Management. Email: 165268650@qq.com		**Xiaofeng Wang** Prof. Engineer. Shanghai Urban Construction Municipal Engineering (Group) Co., Ltd. Research Direction: Bridge and Municipal Engineering Project Construction Management. Email: 279756599@qq.com

AUTHOR BIOGRAPHIES

Xiabin Yuan
CEO. Shanghai Swissdam Environmental Protection Technology Co., Ltd.
Research Direction: Scientific Research, Design Consulting, Construction Management of new materials.
Email: yuanxiabin01@126.com